Active Control of Tip Vortex using HHC and Tab in Helicopter

by
Choongmo YANG, Takashi AOYAMA, and Shigeru SAITIO
Japan Aerospace Exploration Agency (JAXA)

ABSTRACT

The effect of active control using HHC(Higher Harmonic Control) and active tab is numerically analyzed in hover and forward flight conditions of helicopter. The characteristics of tip vortex such as vortex center position, maximum vorticity, core radius are compared according to the flight conditions. A sub-region interpolation method is used to find accurate positions of tip vortex center after calculation. The unsteady oscillation of angle of attack by HHC and the increase of thrust by active tab are enough for controlling the vertical location of tip vortex to increase the miss-distance between a blade and a tip vortex at the BVI event.

1. Introduction

Blade-vortex interaction (BVI) is one of the main noise sources of helicopters. Various kinds of reduction techniques for BVI noise have been proposed. One of them is flight path management and control. Schmitz, et al.[1, 2] developed a quasi-static acoustic mapping (Q-SAM) method to estimate ground noise level trends and indicated that choice of flight path angle, X-Force, and vehicle acceleration has an important influence on the ground noise exposure.

Alternative techniques are passive tip-shape modification[3-6] and active rotor control[7]. The tip-shape modification has been successfully applied for reduction of high-speed impulsive (HSI) noise[8, 9], which is generated by the shock wave on the blade surface on advancing side. This technique works well on the reduction of shock wave strength. However, the reduction of BVI noise by this technique is not expected much. Therefore, active rotor controls, such as higher harmonic control (HHC), individual blade control (IBC), active flap, and so on, are expected to become the breakthrough for dramatic reduction of BVI noise. Research on these techniques is reviewed in Ref. 7 well. JAXA (Japan Aerospace Exploration Agency) and Kawada Industries, Inc. originally devised active tab[10] (Fig. 1) as one of the active techniques. Some experimental investigations of active tab have been conducted by them. The noise reduction effect by active tab has been demonstrated even in a wind tunnel test[11] using a one-bladed rotor without flapping motion. Therefore, the main reason of the noise reduction seems to be the increase of miss-distance between a blade and a vortex mainly caused by the geometrical change of tip-vortex location by active tab.

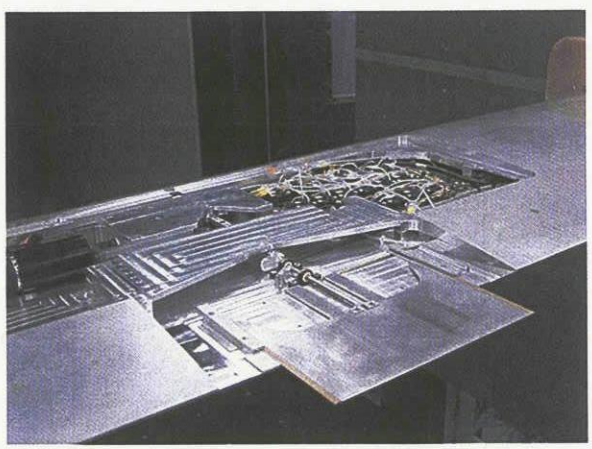

Fig.1: Active tab installed in a blade used for a wind tunnel test10

In the present paper, the effect of active control using HHC(Higher Harmonic Control) and active tab is numerically analyzed in hover and forward flight conditions of helicopter. The objective of this study is to obtain better understandings for the mechanism of noise reduction by active tab using numerical simulation. The effect of tab on rotor thrust, tip vortex, and noise is analyzed and discussed. The characteristics of tip vortex such as vortex center position, maximum vorticity, core radius are compared according to the flight conditions.

2. Numerical Methods

A 3D unsteady Euler CFD[12] code is used for the aerodynamic calculations in the analysis of rotor thrust, tip vortex, and noise. The Euler equations are discretized in the delta form using Euler backward time differencing. A diagonalized approximate factorization method, which utilizes an upwind flux-split technique, is used for the implicit left-hand-side for spatial differencing. For unsteady calculations in forward flight, the Newton iterative method is added in order to reduce residual in each time-step. The number of Newton iteration is 4. Grid generation is conducted in each time step of CFD calculation according to the motion of HHC and active tab. In the analysis of tip vortex, the grid is curved in its wake region as shown in Fig. 2 so that the region of densely distributed grid traces the trajectory of tip vortex to maintain the grid resolution.

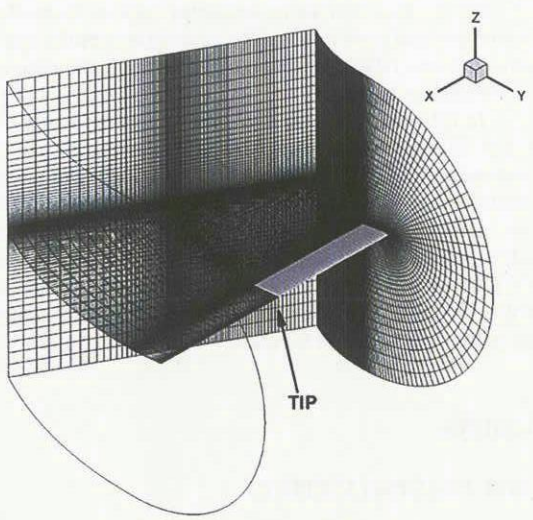

Fig.2: Grid of single blade

Fig. 3 shows the CFD grid around an active tab moving at the trailing-edge of an airfoil section. The number of gird is about 1.16 million in the tip vortex calculation, and about 162 thousand in the noise calculation.

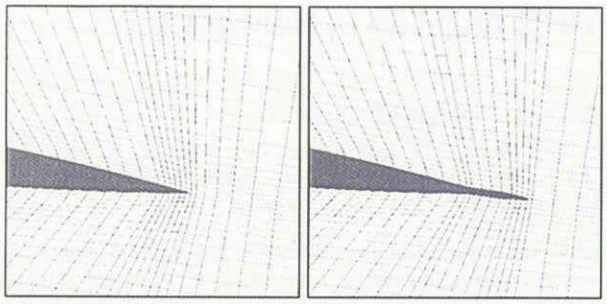

(a) Tab Length =0.0 (b) Tab Length =0.1C

Fig.3: CFD grid of active tab.

The definition of tab angle is given in Fig. 4. The quantity of tab angle has a limitation depending on the space of trailing-edge region for putting back the tab. In the case of NACA0012, tab angle more than 6° may be difficult. The calculations are performed in the condition of M_{tip}=0.65, and α=5°.

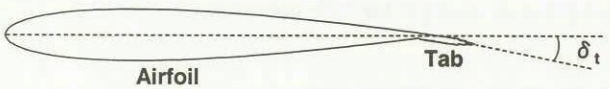

Fig.4: Definition of tab angle

The motion of active tab is defined as $L_t(\psi) = (L_{t0}/2)\cos(P_t\psi - \psi_0)$, where □, L_t(□), L_{t0}, P_t, and □$_0$ are azimuth angle, tab length at □, maximum of tab length, frequency, and phase angle of tab motion. HHC and active tab as active control of tip vortex is analyzed for hovering and forward flight. The motion of HHC is $\theta_{HHC}(\psi) = \theta_0 \cos(P_t\psi - \psi_0)$, where □, □$_{HHC}$(□), □$_0$, P_t, and □$_0$ are azimuth angle, pitch angle at □, amplitude, frequency, and phase angle of HHC motion.

A sub-region interpolation method was used to find accurate positions of tip vortex center after calculation. The unsteady oscillation of angle of attack by HHC and the increase of thrust by active tab are enough for controlling the vertical location of tip vortex to increase the miss-distance between a blade and a tip vortex at the BVI event. However, these active control methods also have some problems such as increasing tip-vortex strength and core radius. The calculation results show that the active tab and HHC affects on the trajectory, the core radius, and the strength of tip vortex.

In this study, calculations are performed using Central Numerical Simulation System (CeNSS), the main part of the third-generation numerical simulator of JAXA. It is composed of high performance UNIX servers, FUJITSU PRIMEPOWER. A crossbar network connects each other of them. CeNSS has 9TFLOPS peak performance, 3TB memory, 50TB disk storage, and 600TB tape archive. It takes about 20 hours to obtain a fully converged solution of a rotor Euler calculation with about 1.16 million grid points using 18 CPUs.

3. Results

VORTEX TRACING METHOD

The center of tip vortex is accurately traced using sub-region interpolation as shown in Fig. 5 by assuming the cubic distribution of fluid properties such as velocity, vorticity, or pressure within a small area (9 points of original grid). The basic interpolation is solved with 3 points in the following equation.

$$\left.\begin{aligned} f(x_1) &= ax_1^{\,2} + bx_1 + c \\ f(x_2) &= ax_2^{\,2} + bx_2 + c \\ f(x_3) &= ax_3^{\,2} + bx_3 + c \end{aligned}\right\} \Rightarrow a, b, c$$

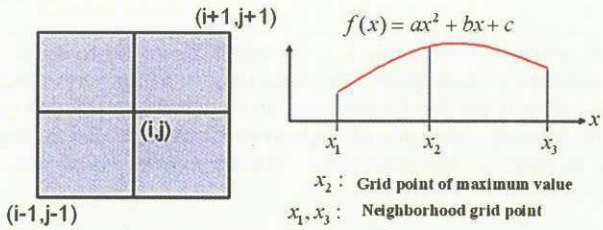

Fig.5: Sub-region interpolation

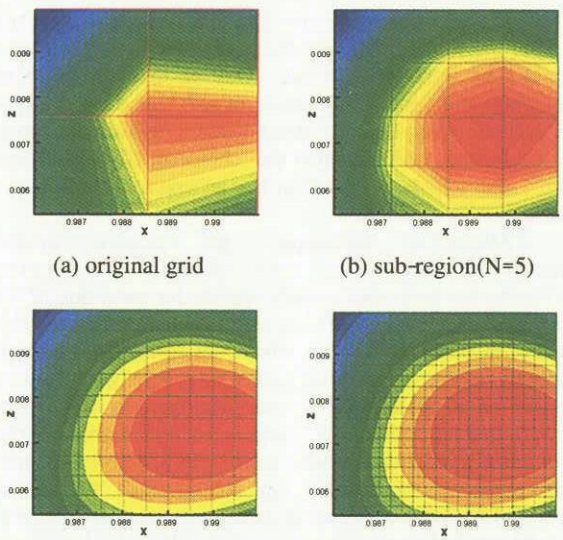

(a) original grid (b) sub-region(N=5)

(c) sub-region(N=10) (d) sub-region(N=20)

Fig.6: Vorticity contours using 2D sub-region interpolation

Fig. 6 shows the vorticity contours interpolated using 2-dimensional sub-region interpolation method with N=3(origin), 5, 10, and 20. Compared to the original grid, the location of vortex center appears more clearly after sub-region interpolation. Fig.7 shows motion of vortex center in hover according to HHC. The irregularity of the trace of vortex center (red line) becomes less to show more smooth motion after sub-region interpolation (blue line).

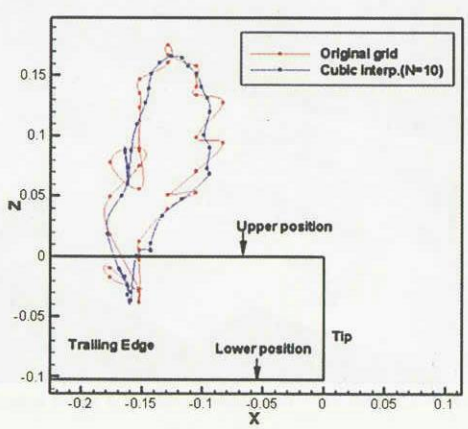

Fig.7: Trace of vortex center at sectional plane along tip vortex

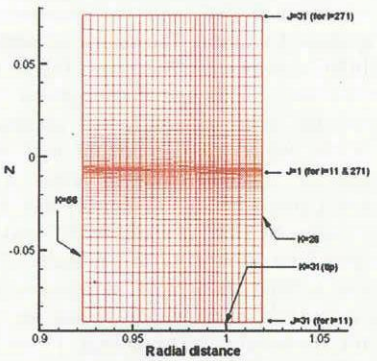

(a) sectional plane in grid system

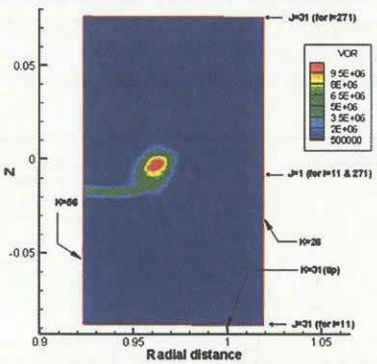

(a) vorticity contour in mid-section

Fig.8: Diagrams of vorticity contour at one sectional plane along a trace of the tip vortex

Fig.8 shows a diagram of sectional plane along the trace of tip vortex and the vorticity contour at that mid-section, which are used in the results.

EFFECT OF ACTIVE TAB ON TIP VORTEX

It is suggested that the increase of thrust by active tab is enough for controlling the vertical location of tip vortex to increase the miss-distance between a blade and a tip vortex at the BVI event. However, the active tab has not only such kind of benefit but also some problems such as increasing tip-vortex strength and core radius. So, the analysis in this section is focused on how much the effect of active tab on the trajectory, the core radius, and the strength of tip vortex is.

Hover

Fig.9(a) shows the series of sectional vorticity contours of tip vortex shed from a blade with active tab in a hover condition. For reference, the result of HHC is also drawn in Fig. 9(b). The motion of HHC is defined as,

$$\theta_{HHC}(\psi) = \theta_0 \cos(P_t\psi - \theta_0),$$

where ψ, $\theta_{HHC}(\psi)$, θ_0, P_t, and θ_0 are azimuth angle, pitch angle at ψ, amplitude, frequency, and phase angle of HHC motion. The characteristics of rotor and the calculation condition are shown in Tables 1 and 2, respectively. This rotor is a modified (no twist) OLS rotor[13]. From these figures, the tab motion remarkably causes the horizontal movement of tip vortex while the HHC motion considerably changes the core radius and the strength of tip vortex.

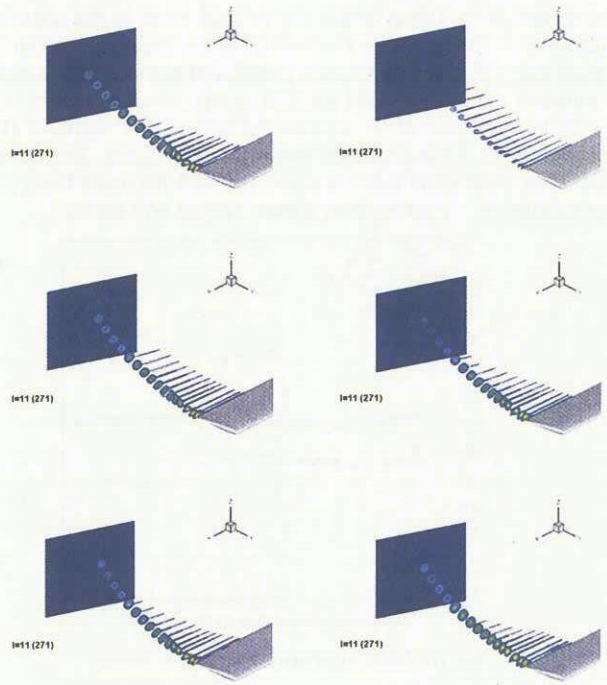

a) Active Tab b) HHC

Fig. 9: Vorticity contour of tip vortex shed from blades with active tab and HHC

Table 1: Characteristics of rotor.

Rotor	
Aspect ratio	9.212
Airfoil	modified BHT540
Twist angle	0.0 deg.
Tip Shape	Rectangular
Number of blade	2

Table 2: Calculation cases.

Condition	
Hover Tip Mach Number	0.664
Collective Pitch Angle [deg.]	5.0
Active Tab	
Max. Length [C]	0.1
Thickness [C]	0.01
Tab Angle [deg.]	0.0 & 5.0
Frequency [/rev.]	3
Phase [deg.]	0.0
HHC	
Amplitude [deg.]	4.0
Frequency [/rev.]	3
Phase [deg.]	0.0

Figure 10 traces the motion of the center of tip vortex on the vertical plane (Trefftz plane) in Fig. 9, which is located at the azimuth of 23° behind the trailing-edge of the blade. The position of vortex center is decided from the CFD solution by finding the maximum point of vorticity magnitude. The horizontal and vertical axes in Fig. 10 indicate span-wise and vertical positions indicated by the percentage of the blade chord length, respectively. The gray circle shows the result without control. The open and black circles are the results of tab angle equal to 0° (Tab A) and 5° (Tab B), respectively. For reference, HHC result is shown by the triangle symbol. In this figure, the vertical position of vortex center is not affected much by Tab A while the span-wise position is dramatically changed. The width of the movement in the span-wise direction reaches about 25% of the blade chord length. Therefore, the active tab seems to affect on the intersection angle between a blade and a vortex at the BVI event. The trajectory of vortex center shifts downward by Tab B

compared with Tab A while the general trend in the span-wise direction is almost same. The bottom of the trajectory of Tab B is more than 4% below the vortex position of non-control. It can be estimated that this bottom position is equivalent to that of HHC with the amplitude of 2° because the bottom of 4°-aplitude HHC shown in Fig. 14 is about 8% below the gray circle. Therefore, it becomes clear again that the active tab with tab angle has a great possibility of increasing miss-distance at the BVI event.

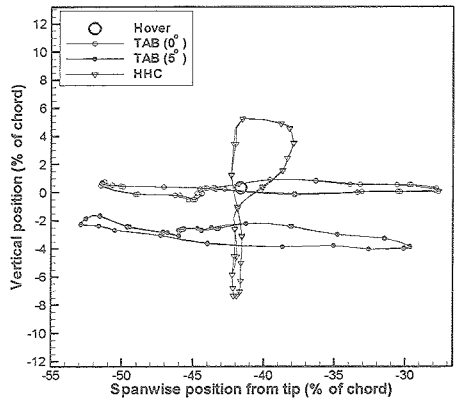

Fig.10: Motion of vortex center in hover.

Fig. 11 shows the variations of core radius of tip vortex, maximum vorticity, and vertical position of vortex center of Tab A on the vertical plane in Fig. 9. The horizontal axis indicates the azimuth-wise position of the blade which sheds the tip vortex. The core radius and the vertical position of vortex center are non-dimensionalized by the blade chord length. The maximum vorticity is non-dimensionalized by the speed of sound in free stream and the blade-span length. The solid, dotted, and gray lines are the results of core radius, vorticity, and vertical position, respectively. For reference, the result of non-control case (baseline) is shown by the straight lines indicated by "Hover". The core radius is the half distance between upper and lower positions of peak velocity where the maximum of the absolute value of velocity component u is observed in the z-axis. The maximum of vorticity is defined as the vorticity magnitude at the vortex center. The variations in Fig. 11 show 3P waves and general trend can be discussed from this figure although the variations include some oscillations due to the difficulty of finding core radius, vorticity, and vertical position from the CFD solutions. This figure indicates that the change of core radius by Tab A is about ±0.4%C from that of the non-control case and the maximum of vorticiy increases up to about 1.2 times as much as that of the non-control case. The change of vertical position is negligible. Therefore, the tab without tab angle is not effective for the reduction of BVI noise because it increases the vortex strength without increasing the miss-distance.

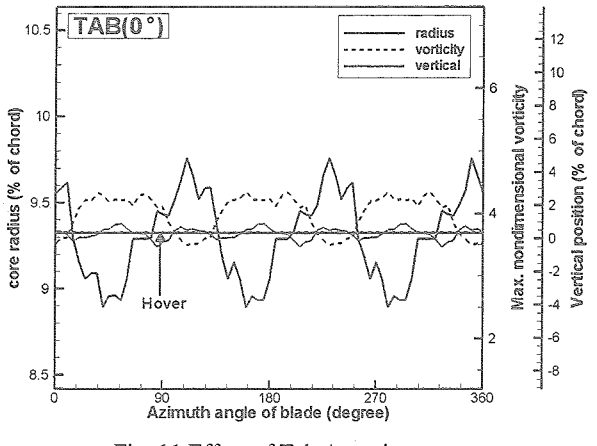

Fig. 11 Effect of Tab A on tip vortex.

In the case of Tab B shown in Fig. 12, the increase of core radius is about 0.6%C and the maximum of vorticiy increases up to about 1.6 times. The change of vertical position is from 2%C to 4%C downward. Therefore, Tab B is effective for increasing miss-distance although it strengthens the tip vortex. Figure 18 shows the result of HHC. It is impossible to obtain core radius in the region of flat bottom indicated by "weak vortex" because the effective angle of attack is too small to generate tip vortex strong enough to identify its core radius. The change of core radius by HHC is about 0.8%C and the maximum of vorticiy varies from about 0.41 to 1.6 times. The change of vertical position is from about 8%C downward to about 5%C upward. An interesting phenomenon is that the peaks of core radius and vorticity are out of phase in Figs. 11 and 12 while they are in phase in Fig. 13. The vorticity is relatively strong in every case when the vertical position is the farthest from the baseline although the maximum of vorticity and the minimum of vertical position are not always in phase. Therefore, the effect of tab and HHC on noise reduction by increasing the miss-distance should be discounted by considering the increase of vortex strength.

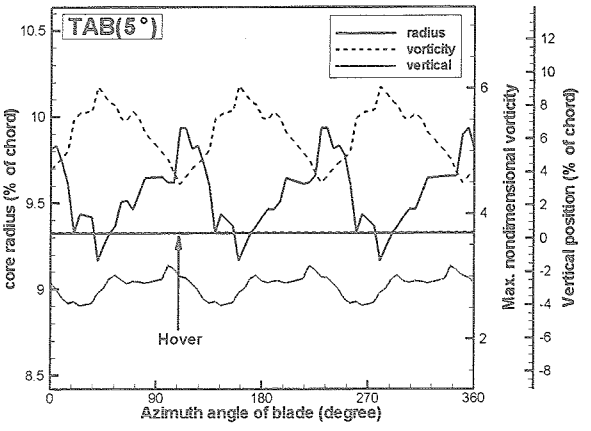

Fig. 12: Effect of Tab B on tip vortex.

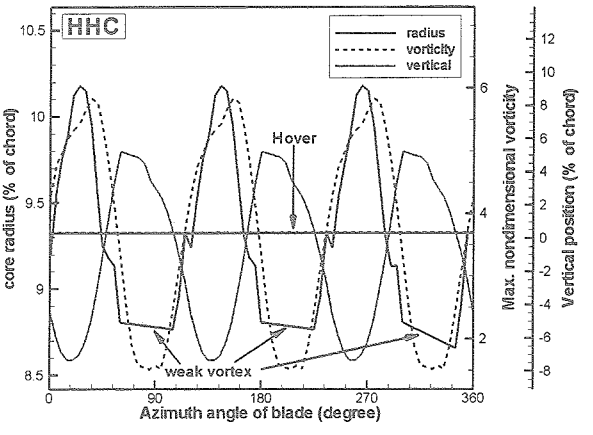

Fig. 13: Effect of HHC on tip vortex.

Forward Flight

The OLS rotor shown in Table 3 is calculated in the condition[16] of Table 4 in order to simulate a realistic helicopter rotor in approach to a landing.

Table 3: Characteristics of rotor.

Rotor	
Aspect ratio	9.212
Airfoil	modified BHT540
Twist angle	10.0 deg. (Linear)
Tip Shape	Rectangular
Number of blade	2

Table 4: Calculation condition.

Condition	
Hover Tip Mach Number	0.664
Freestream Mach Number	0.109
Collective Pitch Angle [deg.]	5.0
Lateral Cyclic Pitch Angle [deg.]	-1.33
Longitudinal Cyclic Pitch Angle [deg.]	2.72

Figure 14 traces the motion of vortex center in the forward flight condition. The open circle shows the result without control (baseline). The dotted and solid lines are the results of Tab A and Tab B, respectively. The symbol of plus indicates the position where the azimuth angle of blade is 0. For reference, HHC result is compared with the baseline result in Fig. 15. The trajectory of Tab B is located downward compared with that of the baseline case while the trajectory of Tab A is almost same as that one. The difference of the bottom position between Tab B and the baseline is about 4%C in the vertical direction. This can stand comparison with the result of HHC in Fig. 15. Therefore, it becomes clear in this forward flight case again that the active tab with tab angle has a great possibility of increasing miss-distance at the BVI event. In addition, the flat bottom of the trajectory obtained by Tab B means the good effect is valid in the wide range of tab motion. The effect of tab on widening the variation of vortex location in the span-wise direction is observed in this forward flight condition like in the hover condition although it is not remarkable because the variation caused by the forward flight velocity is dominant.

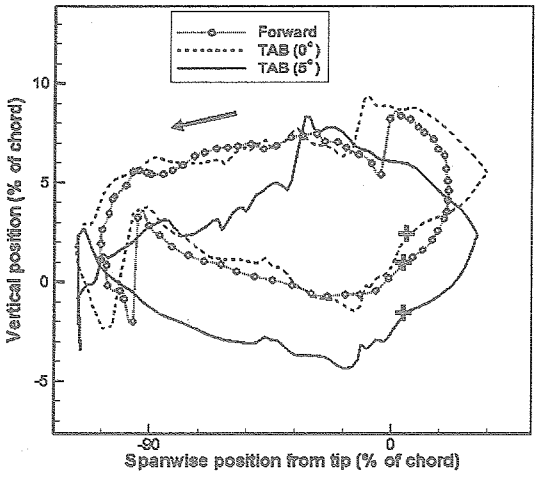

Fig. 14: Motion of vortex center in forward flight (non-control, Tab A, and Tab B)

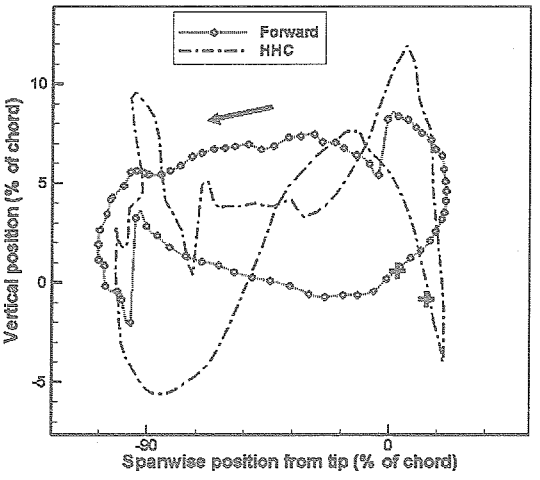

Fig. 15: Motion of vortex center in forward flight (non-control and HHC)

Figure 16 shows the effect of tab and HHC on core radius, vorticity, and vertical position of tip vortex. The gray line indicated by "Forward" shows the result without control (baseline). The dotted and solid lines are the results of Tab A and Tab B, respectively. For reference, HHC result is drawn by the dot-dash line. The result of Tab A is almost same as that of the baseline in every figure. It means that Tab A is not effective for noise reduction. The vertical position of Tab B is always located below that of the baseline case except for the reverse region from 70° to 100° and 240° to 250° of the blade azimuth angle. The difference varies from 2%C to 4%C except for the reverse region. This result is similar to that in the hover case shown in Fig. 12. One of the problems for Tab B is that the vorticity of Tab B is more than that of the baseline case everywhere at the azimuth angle of blade while the vorticity of HHC changes up and down from that of the baseline case according to the 3P motion. Another problem is that Tab B dramatically increases the core radius in some region of azimuth angle of blade. Therefore, more effort to find the appropriate location of tab in blade span and the adequate phase angle of tab motion is required in order to make use of the possibility of increasing miss-distance at the BVI event without increasing vortex strength and core radius much.

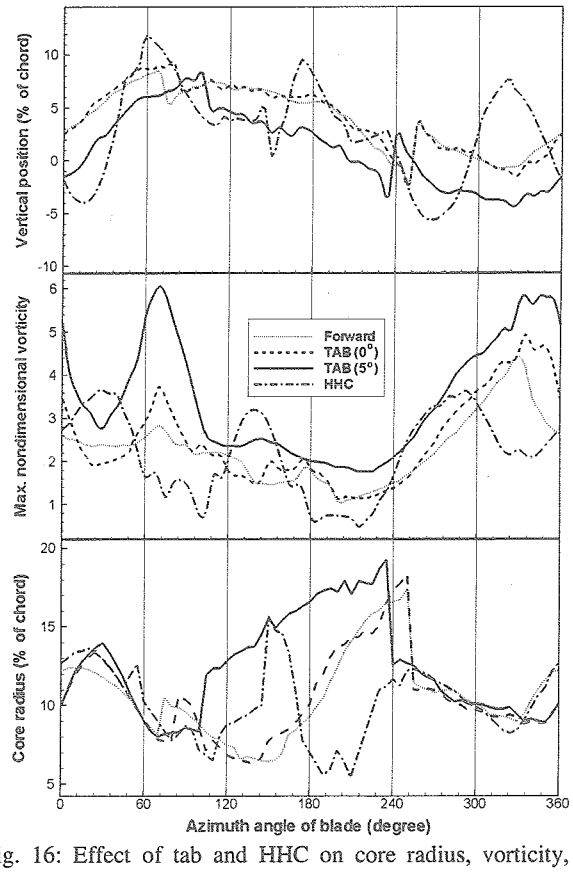

Fig. 16: Effect of tab and HHC on core radius, vorticity, and vertical position of tip vortex.

EFFECT OF ACTIVE TAB ON NOISE

The effect of Tab B on BVI noise is roughly estimated in this section. Figure 17 traces the motion of vortex center of Tab B on three Trefftz planes located at the angle of 18.5°, 23°, and 27.5° behind from the trailing-edge of the blade in the hover condition of Table 2. The open circle indicates the averaged center position of each trace. The result of the baseline case is plotted by the gray circles. The quantity $\Delta_{m.d.}$ is defined as the offset distance between the center of "Hover" and the lowest vortex center of Tab B. This quantity increases as the growth of tip vortex as shown in this figure. When linearly extrapolated to the blade azimuth of 300°, which is the vortex age of generating

severe parallel BVI in the forward flight condition of Table 4, $\Delta_{m.d.}$ reaches to about 0.35C. This value is equivalent to the miss-distance which gives about 7dB reduction of BVI noise according to the results from previous research[14].

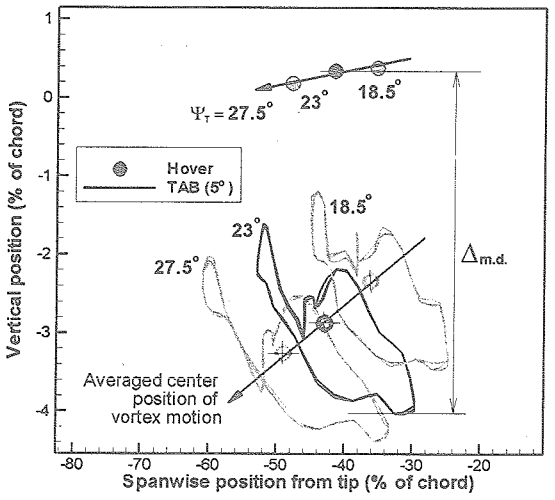

Fig. 17: Motion of vortex center of Tab B and baseline in hover

CONCLUSIONS

A 3D unsteady Euler CFD code was applied to understand the effect of HHC and active tab on tip vortex, and BVI noise. As a result, the followings were found.

1. The motion of active tab with tab angle changes the vertical position of tip-vortex center and its magnitude can stand comparison with the result of HHC. In addition, the tab motion remarkably causes the horizontal movement of tip vortex.

2. A possible reduction of BVI noise by an active tab with tab angle is estimated considering the vertical position of vortex center and the circulation of tip vortex.

The topic of this study covers only a part of the effect of active tab on BVI noise reduction. More comprehensive studies using our advanced CFD code[15] will be performed in the next step. Moreover, Navier-Stokes analysis is required for more accurate discussion on the phenomenon related to the tip vortex.

References

1) Gopalan, G., Schmitz, F. H., and Sim, B. W., Flight Path Management and Control Methodology to Reduce Helicopter Blade-Vortex Interaction (BVI) Noise, AHS Vertical Lift Aircfraft Design Conference, San Francisco, CA, Jan., 2000.
2) Schmitz, F. H., Gopalan, G., and Sim, B. W., Flight Trajectory Management to Reduce Helicopter Blade-Vortex Interaction (BVI) Noise with Head/Tailwind Effects, 26th ERF, No. 77, The Hague, The Netherlands, Sep., 2000.
3) Boxwell, D. A. and Schmitz, F. H., Full-Scale Measurements of Blade-Vortex Interaction Noise, Journal of the American Helicopter Society, Vol.27, (4), Oct, 1982, pp.11-27.
4) Martin, R. M. and Connor, A. B., Wind-Tunnel Acoustic Results of Two Rotor Models with Several Designs, NASA-TM 87698, 1986.
5) Yu, Y. H., Liu, S. R., Jordan, D. E., Landgrebe, A. J., Lorber, P. F., Pollack, M. J., and Martin, R. M., Aerodynamic and Acoustic Test of a United Technologies Model Scale Rotor at DNW, AHS 46th Annual Forum, May, 1990.
6) Lowson, M. V., Progress Towards Quieter Civil Helicopters, 17th ERF, No. 59, 1991.
7) Yu, Y. H., Gmelin, B., Splettstoesser, W., Philippe, J.J., Prieur, J., and Brooks, T., Reduction of Helicopter Blade-Vortex Interaction Noise by Active Rotor Control Technology, Prog. Aerospace Sci., Vol. 33, 1997, pp. 647-687.
8) Baeder, J. D., Passive Design for Reduction of High-Speed Impulsive Rotor Noise, AHS 52nd Annual Forum, Washington DC, June 1996.
9) Aoyama, T., Aoki, M., Kondo, N., Saito, S., and Kawachi, K, Effect of Blade-Tip Shape on High-Speed Rotor Noise, AIAA Paper 96-2380, June 1996.
10) Kobiki, N., et al., Active Tab, a New Active Technique for Helicopter Noise Reduction, 29th ERF, 2003.
11) Kobiki, N., Akasaka, T., Kondo, N., Tanabe, Y., and Saito, S., An Experimental Study of On-blade Active Tab for helicopter noise reduction, 30th European Rotorcraft Forum, September 2004.
12) Aoyama, T., et al., Unsteady Calculation for Flowfield of Helicopter Rotor with Various Tip Shapes, 18th European Rotorcraft Forum, Paper No.B03, Avignon, France, September 1992.
13) Splettstoesser, W. R., Schultz, K. J., Boxwell, D. A., and Schmitz, F. H., Helicopter Model Rotor Blade Vortex Interaction Impulsive Noise: Scalability and Parametric Variations, 10th European Rotorcraft Forum, Paper Nr.18, 1984.
14) Aoyama, T., Kondo, N., Fukagawa, A., and Saito, S., Effect of Rotor Rotational Speed on Blade-Vortex Interaction Noise, Inter Noise 2003, N1013, Korea, August 2003.
15) Ochi, A., Aoyama, T., Saito, S., Shima, E., and Yamakawa, E., BVI Noise Predictions by Moving Overlapped Grid Method, AHS 55th Annual Forum, Montreal, Canada, May 1999